

## SSC21-WKII-01

**Development of Formation Flying CubeSats and Operation Systems  
for the CANYVAL-C Mission: Launch and Lessons Learned**

Geuk-Nam Kim, Sang-Young Park, Taeyang Lee, Dae-Eun Kang, Namgyu Kim,  
Soobin Jeon, Eunji Lee, Youngbum Song  
Department of Astronomy, Yonsei University, Seoul, Republic of Korea  
Yonsei University, 50 Yonsei-ro, Seodaemun-gu, Seoul, Republic of Korea; +82 2 2123 4442  
[south1003@yonsei.ac.kr](mailto:south1003@yonsei.ac.kr)

**ABSTRACT**

The CubeSat Astronomy NASA and Yonsei using Virtual telescope ALignment for Coronagraph (CANYVAL-C) is a technology demonstration mission that shows the concept of a virtual space telescope using two CubeSats in formation flying. The final goal of the mission is to obtain several images of the solar corona during an artificial solar eclipse created by the two CubeSats, Timon (1U CubeSat) and Pumbaa (2U CubeSat). To implement this mission, two CubeSats in formation flying and a ground segment have been developed. The CubeSats were constructed mainly with commercial off the shelf components, sharing the bus architecture. The payload of each CubeSat is a visible camera and an occulter to block the light from the photosphere of the Sun. The occulter is composed of tape measures and a black-colored polyimide film; the system size is smaller than 0.5U ( $10 \times 10 \times 5 \text{ cm}^3$ ) while it stowed and enlarged to  $0.75 \times 0.75 \text{ m}^2$  after spreading the film. The 3D-printed propulsion system is smaller than 0.5U and facilitates accurate positioning maneuvers of Pumbaa. The on-board computer has multi-task processing capabilities and a space-saving configuration which is integrated with the GNSS receiver and the UHF transceiver. The core technology for the mission implementation is the precise formation flying guidance, navigation, and control system with a cold-gas propulsion system and an inter-satellite link system. The specification of each CubeSat system was evaluated using numerical simulations and ground testing. To operate CubeSats, the ground segment was constructed with some components, including the UHF ground station (UGS), flight dynamics system (FDS), mission analysis and planning system (MAPS), and spacecraft operation system (SOS). Each component works under the environment of an integrated graphic user interface. In particular, the UGS handles the RF communication, data storage, and instrument control for tracking CubeSats. The FDS processes the navigation data to precisely estimate absolute position and velocity. Then, the MAPS determines the allowable mission schedule and parameter set for implementing maneuvers of each CubeSat. Using the MAPS, feasibility of the mission operation can be ensured through numerical simulations based on the solutions from the FDS. Finally, the SOS is the interface system between each component, processing telemetry and generating telecommand. The CubeSats were launched on March 22, 2021, by Soyuz-2.1a with a Fregat stage.

*Keywords:* Formation Flying, Virtual Space Telescope, Solar Corona.

**INTRODUCTION**

A virtual space telescope (VT) is a promising concept to enhance observational performance of conventional space telescopes. The VT is composed of a detector and optics systems based on the formation flying technologies of two or more spacecrafts. The separated structure can extend the focal length significantly, providing high-quality celestial images especially in X-ray region.<sup>1,2</sup> To establish the VT, the detector and optics systems should be aligned remotely with respect to a celestial target, defined as the inertial alignment hold (IAH) technology. Yonsei University and NASA/GFSC proposed the CANYVAL (CubeSat Astronomy NASA and Yonsei using Virtual telescope ALignment) project to implement technologies for the VT in space.

The CANYVAL-C (Coronagraph) mission is the follow-up mission of the CANYVAL-X (eXperiment) mission. The final goal of the mission is to obtain several images of the solar corona by constructing an artificial solar eclipse with two CubeSats. Figure 1 shows the concept of the CANYVAL-C mission. The CubeSat Yonsei team developed the CubeSats and the ground segment. The 1U CubeSat, named Timon, includes a visible camera. The 2U CubeSat, named Pumbaa, includes a deployable device to completely block the sunlight, called the occulter. Given the limitation in resources involved in the size, weight, and power (SWaP), miniaturized and low-power-consumption components were developed, such as the occulter, propulsion system, and on-board computer (OBC). The core technologies for the mission implementation are the

guidance, navigation, and control (GNC) systems for precise formation flying, a cold gas propulsion system, and the inter-satellite link (ISL) system.<sup>3</sup> The ground segment has been developed in Yonsei University, Seoul, to operate CubeSats, including the UHF ground station (UGS), flight dynamics system (FDS), mission analysis and planning system (MAPS), and spacecraft operation system (SOS). The CubeSats were launched on March 22<sup>nd</sup>, 2021, by Soyuz-2.1a with a Fregat stage at Baikonur cosmodrome.

This paper presents the introduction of the CANYVAL-C mission, development of CubeSat and operation systems, and lesson learned from the initial identification attempt.

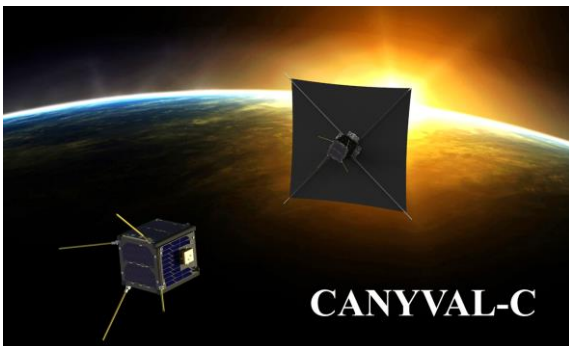


Figure 1: Illustration of the CANYVAL-C mission<sup>3</sup>

## CANYVAL-C MISSION

### Mission Requirements

The primary objective of the mission is to obtain images of the solar corona during an artificial solar eclipse created by two CubeSats. While capturing images, Timon should be placed in the umbra generated by the occulter. Furthermore, the field of view (FOV) of the camera should cover the solar corona region with an angular diameter 10 times that of the solar angular diameter. To accomplish these conditions, the relative positioning maneuver, termed the IAH, is performed with respect to the Sun.

Table 1: Mission Requirements and Constraints

Content	Description
Constraint	(1) 20 ~ 53 m for the relative distance (2) Two CubeSats is contained in a single deployer
Relative positioning	(1) < 5 m ( $3\sigma$ ) for the sphere radius (2) < 7.5° ( $3\sigma$ ) for the alignment angle
Payload specification	(1) > 30° for the camera system's FOV (2) > 0.5 × 0.5 m <sup>2</sup> for the deployed occulter size

Table 1 summarizes the mission requirements and constraints. First, to prevent collision of the CubeSats with each other and to allocate the size of the occulter, the relative distance is constrained from 20 to 53 m. In addition, given the available deployer size for the project, the two CubeSats are contained in the same deployer, complying with the system sizing and configuration requirements. The requirements of the IAH are as follows; the relative position errors should be restricted to less than 5 m of the sphere radius ( $3\sigma$ ), given a relative distance of 40 m with the base line; the alignment errors should be restricted to less than 7.5° ( $3\sigma$ ). The alignment angle is defined as the angle between the relative position vectors and vector from Timon to the Sun. The inaccurate alignment induces a degradation of the image quality as shown in Figure 2. Finally, the required specifications for the payload are derived with the given constraints and requirements. The camera on Timon should have a wide FOV, which is larger than 30°. Then, the occulter on Pumbaa should have an area of 0.5×0.5 m<sup>2</sup>.

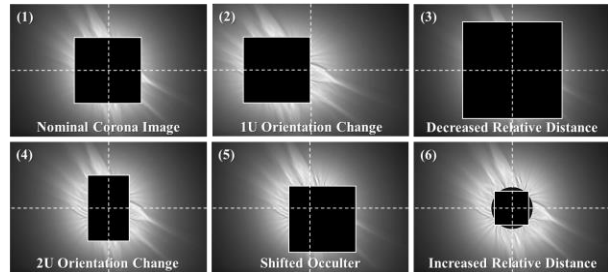


Figure 2: Expected solar corona images from Timon's view<sup>3</sup>

### Concept of Operations

During a mission lifetime of 6 months, the mission consists of the launch and early orbit phase (LEOP), drift recovery and station keeping phase (DRSK), and autonomous formation flying phase (AFFP). Figure 3 depicts the concept of operations for the CANYVAL-C mission from the launch to the end of life.

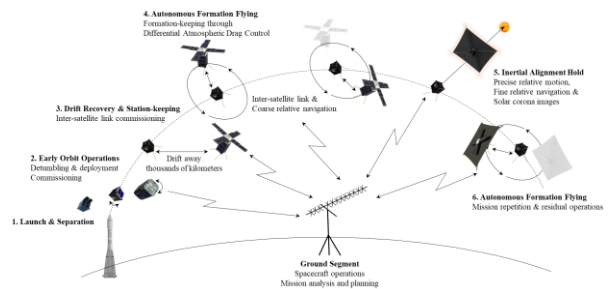


Figure 3: Concept of operations for the CANYVAL-C mission<sup>4</sup>

In the LEOP, after detumbling and the first contact, operations of system commissioning are performed. Although perturbations cause the two CubeSats to drift away from each other, the relative distance can be recovered by utilizing the propulsion system on Pumba during the DRSKP. The maneuvers are repeated until the relative distance is less than 10 km, when the ISL can be established. After the DRSKP, the two CubeSats autonomously maintain the relative distance within few kilometers via the differential atmospheric drag control (DADC)<sup>5</sup>. Additionally, in the AFFP, two types of relative navigation, termed as the coarse mode and fine mode, are performed to determine Pumbaa's relative states with respect to Timon. For the rendezvous (RDV) and the IAH, the fine mode based on the differential GPS (DGPS) algorithm<sup>6</sup> is executed to meet requirements of the relative navigation, within 1 m ( $3\sigma$ ) on each axis.

## CUBESAT SYSTEMS

The payload of Timon is the camera system with a commercial CMOS sensor and a lens. The FOV is  $33.4^\circ \times 43.5^\circ$ , extending coverage to the exterior solar corona region. Additionally, the occulter of Pumba enables to block the sunlight with an extremely low transmittance, dimmer than the light intensity of the solar corona. The occulter is composed of tape measures and a black-colored polyimide film; while the occulter is stowed, the size is smaller than 0.5U, and it is enlarged to  $0.75 \times 0.75 \text{ m}^2$  once the film is spread.

Given the limitation in resources, miniaturized and low-power-consumption components are developed such as the occulter, the propulsion system, and the OBC. Most subsystems of the CubeSats were constructed with the commercial off the shelf (COTS) components. They share the bus architecture including electrical interfaces, enabling fast development. Especially, two-wire interfaces like CAN-bus and I<sup>2</sup>C facilitate easy integration of the systems with reduced amount of wiring. Furthermore, the OBC is integrated with the GNSS receiver, UHF transceiver, and several attitude sensors to save internal space. The communication system enables the uplink, downlink, and ISL with a single UHF transceiver.<sup>4</sup>

### Specifications of Timon (1U CubeSat)

Figure 4 and Table 2 describe the configurations and specifications of Timon, respectively. From the total ionization dose (TID) simulations using the SPENVIS, the cosmic ray accumulation on internal components is predicted as 6.83 krad over 1 year, which is three times smaller than the radiation tolerance of the electronics. Timon utilizes 3-axis magnetic torquers for attitude control. The attitude estimation is based on the EKF, for

which the measurement data is provided by a fine Sun sensor, an inertial measurement unit, and magnetometer. While capturing the solar corona images and charging the battery, Timon should have a pointing accuracy less than  $5^\circ$  with respect to the Sun. Body-mounted solar panels on each axis generate approximately 2 W power in an orbit average. The RF link margin is 3.8 dB for downlink with  $20^\circ$  of elevation.

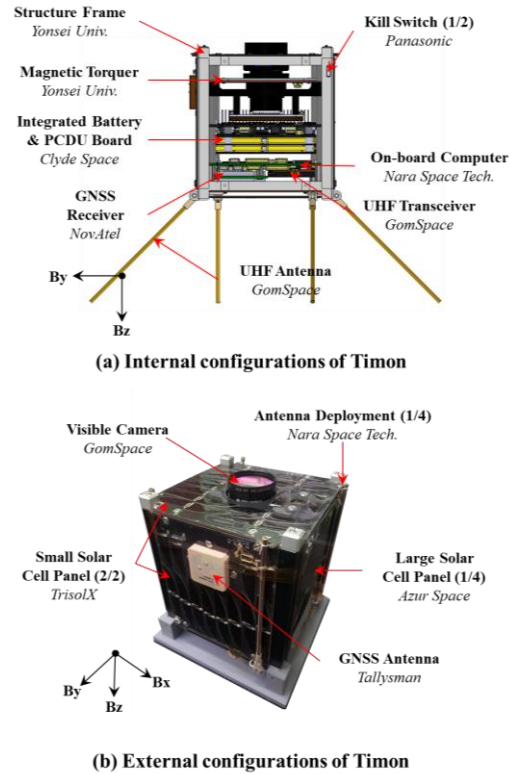


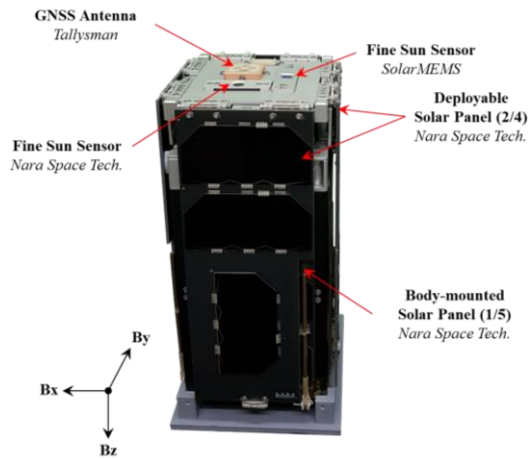
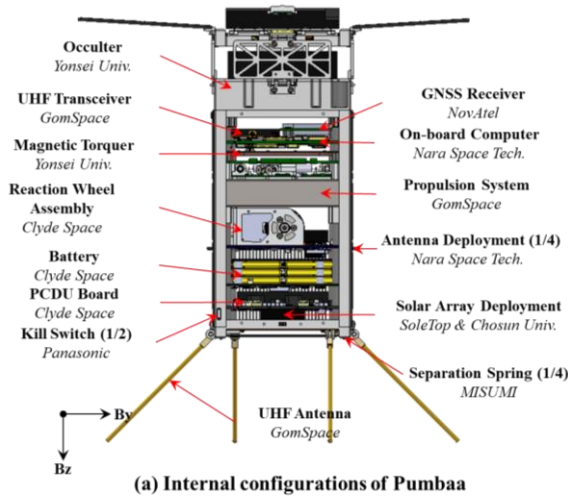
Figure 4: Configurations of Timon

Table 2: Specifications of Timon

Contents	Requirements	Specifications
Systems lifetime	> 6 months	18 months
Payload	> $30.0^\circ$	$33.4^\circ \times 43.5^\circ$
Attitude control ( $3\sigma$ )	> $5^\circ$ (sun-pointing) > $0.5^\circ/\text{s}$ (normally)	$2.9^\circ$ $0.2^\circ/\text{s}$
Link margin	> 3 dB	3.8 dB
Uplink	> 2.4 kbps	4.8 kbps
Downlink	> 4.8 kbps	9.6 kbps
Inter-satellite link	> 4.8 kbps	9.6 kbps
Power generation	> 1.6 W (orbit average power)	2.0 W
Mass	< 1.33 kg	1.09 kg
Deployment	-	UHF Antenna

**Table 3: Specifications of Pumbaa**

Contents	Requirements	Specifications
Systems lifetime	> 6 months	18 months
Payload film	> 0.5 × 0.5 m <sup>2</sup>	0.75 × 0.75 m <sup>2</sup>
Relative navigation & positioning (3σ)	< 1 m (each axis) < 3 m (each axis)	[0.25, 0.44, 0.40] m [2.97, 2.98, 2.86] m
Attitude control (3σ)	> 3° (sun-pointing) > 0.5°/s (normally)	1.8° 0.2°/s
Link margin	> 3 dB	3.8 dB
Uplink	> 2.4 kbps	4.8 kbps
Downlink	> 4.8 kbps	9.6 kbps
Inter-satellite link	> 4.8 kbps	9.6 kbps
Power generation	> 4.0 W (orbit average power)	5.1 W (normally) 8.3 W (sun-pointing)
Stiffness	> 40 Hz (1 <sup>st</sup> mode)	> 76.9 Hz
Mass	< 2.66 kg	2.56 kg (wet)
Deployment	-	UHF Antenna, Solar Panels, Occulter



**Figure 5: Configurations of Pumbaa**

**Specifications of Pumbaa (2U CubeSat)**

The configurations and specifications of Pumbaa are presented as Figure 5 and Table 3, respectively. Pumbaa performs precise attitude control and orbit maneuver utilizing 3-axis reaction wheels and the cold gas propulsion system, respectively. The sub-meter level relative navigation presented by the system meets the requirements. In addition, from the Monte-Carlo simulations, the relative positioning system is evaluated, presenting a positioning error within 3 m on each axis. Deployable solar panels provide electrical power sufficiently to operate high-power-consumption actuators. Although Pumbaa has flexible components with a deployment mechanism, the 1st mode natural frequency is higher than 70 Hz on the y-axis deployable solar panel.

**Assembly, Integration, and Testing**

The CubeSats were developed following the proto-flight model (PFM) philosophy. They were evaluated through numerical simulations and on-ground testing including end-to-end (ETE) testing, day-in-the life (DIL) testing, and environment testing.<sup>4</sup>

Figure 6 shows the setting for the ETE and DIL testing for Timon, including the simplified UHF ground station. The CubeSats were operated with a software for the ground station, following operation scenarios. The autonomy of the flight software (FSW) was assured by monitoring real-time operation over one day. Specially, the emergency mode was evaluated by providing predefined anomalies, including a failure of antenna deployment in the LEOP, a fault of the gyro sensor, and uploading wrong telecommands.



**Figure 6: Example of setting for end-to-end and day-in-the life testing**



The launch environment testing was conducted to evaluate the structural stiffness from acceleration and random vibration of the launch vehicle, Soyuz-2.1a with a Fregat stage. The responses of the acceleration sensor on each axis are presented in Figure 7. Large changes in the natural frequency and responses before/after testing occurred at deployable solar panels. From the visual inspections, it was concluded that the changes were induced by loosen nylon wires on the panels.

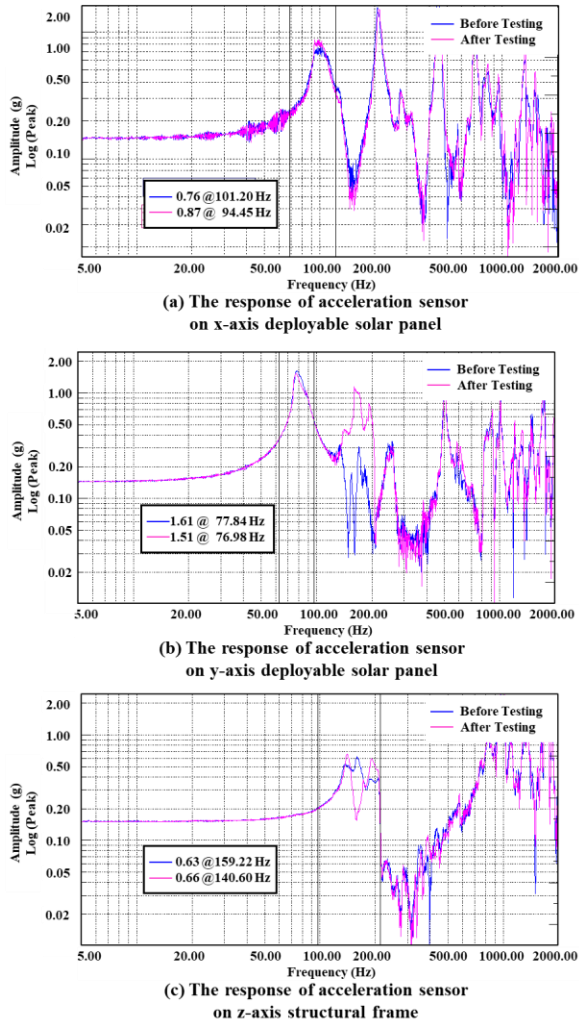


**Figure 7: Response of acceleration sensors on each axis for launch environment testing**

Given the operational and survival temperature range of the electronics, space thermal environment testing was conducted. The temperature range for testing was predicted to be from from  $-15$ – $30^{\circ}\text{C}$  through on-orbit thermal analysis. Figure 8 presents the temperature profiles of the thermo couples (TCs) attached on each panel. At the highest and lowest temperatures, functional testing was executed and the performance of the heaters on the battery and propulsion system was

evaluated. From the results, it is concluded that the heaters on the propulsion system enable to fire in eclipse; in addition, the power budget for the heaters was estimated.

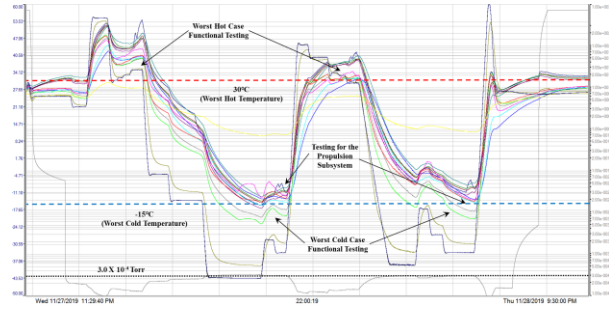


**Figure 8: Temperature profiles of the TCs**

## OPERATION SYSTEMS

The ground segment located at Yonsei University, Seoul, is composed of the UHF ground station, FDS, MAPS, and SOS as shown in Figure 6. The UHF ground station is developed with C language in a Linux environment. All systems are implemented with a graphic user interface (GUI). It handles the RF communication, data packet, and the instrument for tracking CubeSats. The SOS is an interface system among UHF ground station, FDS, and MAPS, which processes telemetry and generates telecommands. The FDS and MAPS are developed using MATLAB in a Windows environment. The General Mission Analysis Tool (GMAT) is applied as a main propagator. On the FDS, the GNSS navigation data are processed to precisely estimate the absolute position and velocity of each CubeSat. Then, the MAPS provides the SOS with the allowable mission schedule and parameter set for implementing maneuvers. Feasibility of the mission operation can be assured through numerical simulations on the MAPS.

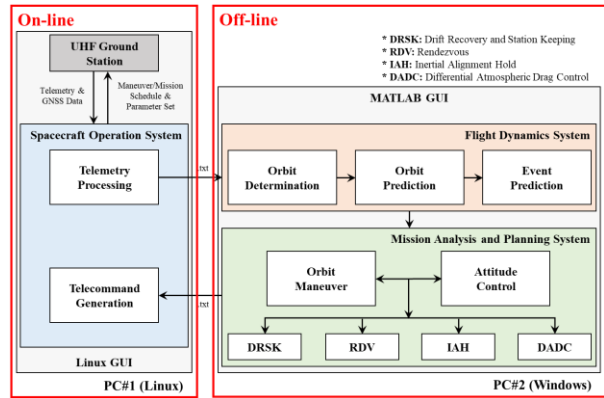


**Figure 6: Ground segment architecture**

### UHF Ground Station (UGS)

The configuration of the UGS is presented in Figure 7. A Yagi antenna is assembled with a rotator to rapidly track the CubeSats. The GS100 transceiver of GomSpace is utilized, which is compatible with the transceivers on the CubeSats. A low noise amplifier (LNA) increases the received signal power up to 20 dB. As the transceivers are of half-duplex type and only have one antenna, they are required to switch between transmission (Tx) and reception (Rx) modes. The RF S/W controller provides the functions to handle Tx and Rx signals, even with signal delays.

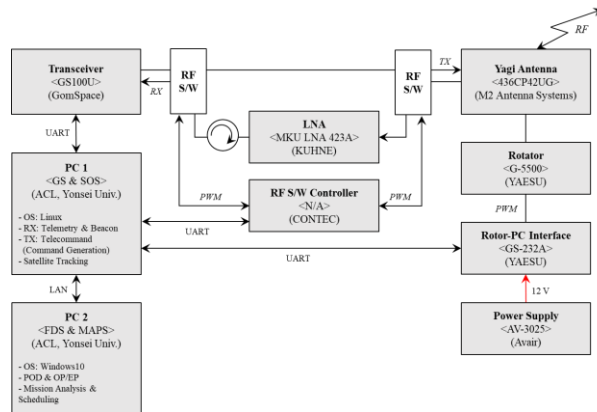


Figure 7: Configurations of the UGS

### Flight Dynamics System (FDS)

The FDS is composed of the orbit determination (OD), orbit prediction (OP), and event prediction (EP) modules.

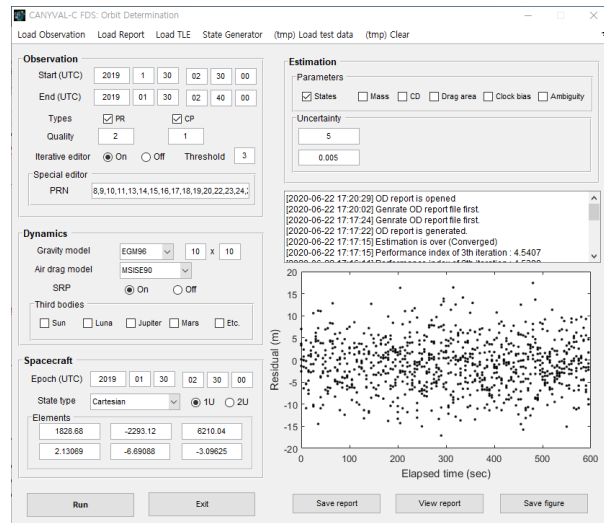


Figure 8: Example of the FDS GUI (OD module)

Given the dynamics and physical properties of each CubeSat, the OD module estimates the state errors at each epoch. The observation data comprise GPS L1 measurement data or the two-line element (TLE). Using the SimGEN data, the OD performance was evaluated, presenting 3 m (3D RMS) for the position error. The OP over 1 day shows less than 500 m (3D RMS), meeting a requirement of 1 km. The EP predicts the eclipse and communication schedule with 1 s of accuracy.

### Mission Analysis and Planning System (MAPS)

The MAPS is developed for scheduling on-orbit operations following the operation scenarios. It consists of five modules including the drift recovery and station keeping (DRSK), differential atmospheric drag control (DADC), rendezvous (RDV), inertial alignment hold (IAH), and the attitude control (AC) modules. They use the results from the FDS.

The DRSK module provides a simulator to analyze maneuver scenarios from current to final burns with the state vectors calculated from the FDS. The firing duration and thrust vector profiles are obtained for each burn. Figure 9 shows the GUI of the DRSK module on the MAPS. The other modules also provide functions for simulation and parameter calculation before generating telecommands. Especially, the AC module calculates the effective projected area based on 3D CAD models of each CubeSat, thus enabling implementation of a precise orbit propagation.

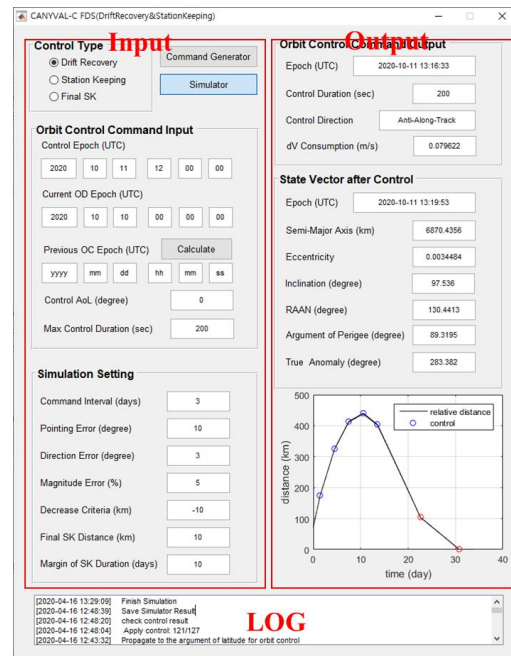


Figure 9: Example of the MAPS GUI (DRSK module)

### Spacecraft Operation System (SOS)

The SOS provides the telemetry to the FDS in a binary format. After the MAPS calculates the mission schedule and configurable parameters, the SOS generates telecommands. Moreover, it integrates the systems of the ground segment using the GUI, including a function of doppler shift correction, ping-pong connectivity, antenna tracking, and visualization as shown in Figure 10. It is possible to simply select several pre-defined telecommands such as those pertaining to changing scenarios and handling anomalies with drag-and-drop actions.

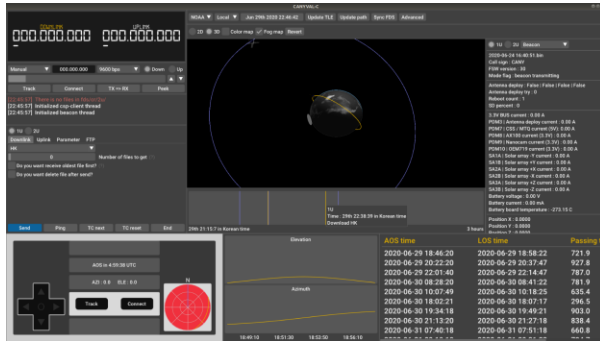


Figure 10: Example of the SOS GUI

### LAUNCH & LESSONS LEARNED

#### Initial Identification Attempt

The CubeSats have been in orbit with 37 satellites, including 29 small satellites since March 22<sup>nd</sup>, 2021. The CubeSat Yonsei team have attempted to identify the CubeSats by operating the ground segment. However, they have been unable to communicate with either CubeSats utilizing the Yonsei ground station. Several amateur ground stations provide signal data and waterfalls through a community such as the SatNOGS. The CubeSat Yonsei team continue their efforts in identifying with the CubeSats, analyzing beacon-like signals received at oversea ground stations.

#### Failure Analysis and Actions

According to the initial identification attempt and problem reports during the CubeSats development lifecycle, the potential reasons for failure are summarized in Table 4. The likelihood and consequence of each reason are analyzed as shown in Figure 11. Although cases of F1, F2, and F9 are less likely to occur, they have the greatest failure impact because communication with the CubeSats will be completely disrupted. Then, action plans are devised to mitigate the failure likelihood, as summarized in Table 5. The actions have been performed over passes.

Table 4: Potential reasons for initial identification failure

ID	Description
F1	Malfunctions of power systems due to kill switch or harness damages from the launch environment
F2	Systems shut-down due to low power margin
F3	Systems booting failure due to OBC malfunctions
F4	Factory reset of CubeSat transceiver due to CubeSat transceiver's FRAM malfunctions
F5	Fail to deploy UHF antenna
F6	Mismatched switching schedule Tx-Rx between ground- and satellite-transceivers
F7	Signal distortions by other satellites signals and ground noise environment
F8	Fail to transmit beacon signals due to the FSW failure
F9	Permanent mechanical and electrical damages on satellite transceiver from the launch and space environment

		Consequence				
		1	2	3	4	5
Likelihood	5					
	4					
	3		F5			F2
	2	F8	F3, F7	F6	F4	F1
	1					F9

Figure 11: Matrix of failure analysis

Table 5: Actions to mitigate the failure likelihood

ID	Action
F1	No actions are available
F2	No actions are available
F3	Autonomous recovery by watchdog timer on EPS modules
F4	Try to communicate with default parameter set
F5	Try to upload telecommand for antenna deployment
F6	Try to change Tx-Rx switching schedule and packet size
F7	Try to receive signals using other sensitive receivers
F8	Try to communicate with candidate parameter set
F9	No actions are available

## Lessons Learned

Given the practical constraints on the development schedule and financial budget for the CANYVAL-C mission, it was possible to construct the CubeSat systems quickly by sharing the bus architecture, including electrical interfaces. Applying the COTS products, more systems level verifications were carried out, including ETE and DIL testing. Although the on-ground verifications enhanced the systems' reliability, there were several potential risks that could induce a system failure.

Considering the aforementioned potential reasons of failure, the lessons learned are summarized as follows. First, the systems should be optimized by simplifying the architecture and operations scenario within the system budget. When constructing the CubeSat systems using standardized COTS products, it is difficult to allow a sufficient system margin. In addition, complicated scenarios might induce uncertainties in power budget analysis. Second, the development of the structure and thermal model (STM) and the engineering model (EM) is recommended to mitigate fatigue of components owing to numerous on-ground testing operations. To increase the success rate and ensure system reliability, more on-ground verifications are required. However, when the PFM philosophy is adopted to construct the CubeSat systems, component level testing might cause a degradation of system performance owing to fatigue. Finally, the LEOP scenarios should be designed to identify the CubeSats quickly and handle anomalies autonomously. Most small satellites are launched with several other satellites to reduce the launch cost, making initial identification difficult owing to RF signals from other satellites before sufficient separation each other. A short interval of beacon transmission might enhance the probability and reduce the time for the first contact.

## CONCLUSION

This paper presents the CANYVAL-C mission concept and its configurations including the CubeSats and the ground segment. In addition, the lesson learned from the initial identification attempt are described along with failure analysis. The CANYVAL-C mission involves demonstrating solar science by implementing formation flying with two CubeSats and obtaining a solar corona image. Verifications of each CubeSat system were conducted to evaluate whether specifications meet requirements. Timon and Pumbaa were launched on March 22<sup>nd</sup>, 2021. Then, in-orbit operations have been attempted by manipulating the developed ground segment. The system architecture,

design process, and lessons learned will contribute to implementation of low-cost and advanced space missions based on formation flying technologies, including next-generation virtual space telescopes.

## Acknowledgments

This work was supported by the Space Basic Technology Development Program through the National Research Foundation (NRF) of Korea, funded by the Ministry of Science and the ICT of the Republic of Korea (NRF-2017M1A3A3A06085349).

## References

1. Shah, N., Calhoun, P.C., Dennis, B.R., Krizmanic, J.F., Shih, A.Y. and Skinner, G.K., "The Virtual Telescope Demonstration Mission (VTDM)", Proceedings of 5th International Conference on Spacecraft Formation Flying Missions and Technologies, Munich, 2013, pp. 1, 15.
2. Park, S.Y., Calhoun, P.C., Shah, N. and Williams, T.W., "Orbit Design and Control of Technology Validation Mission for Refractive Space Telescope in Formation Flying", AIAA Guidance, Navigation, and Control Conference, Mayland, 2014, pp. 13, 17.
3. Kim, G.N., Park, S.Y., Kang, D.E., Son, J., Lee, T., Jeon, S., Kim, N. and Park, Y.K. "Development of CubeSats for CANYVAL-C Mission in Formation Flying", Proceedings of the Asia-Pacific International Symposium on Aerospace Technology, Gold Coast, 2019, pp. 813, 824.
4. Kim, G.N., Park, S.Y., Lee, T., Kang, D.E., Jeon, S., Son, J., Kim, N., Park, Y.K. and Song, Y., "Development of CubeSat Systems in Formation Flying for the Solar Science Demonstration: the CANYVAL-C Mission," Submitted to Advances in Space Research, January 2021.
5. Lee, Y., Park, S.Y., Song, Y. and Park, J.P. "Numerical Analysis of Relative Orbit Control Strategy of CANYVAL-X Mission", Journal of Astronomy and Space Sciences, Vol. 36, No. 4, 2019, pp. 235, 248.  
doi: 10.5140/JASS.2019.36.4.235
6. Leung, S. and Montenbruck, O., "Real-Time Navigation of Formation Flying Spacecraft Using Global Positioning System Measurements", Journal of Guidance, Control, and Dynamics, Vol. 28, No. 2, 2005, pp. 226, 235.  
doi: 10.2514/1.7474